Magazine of Civil Engineering

ISSN 2712-8172

journal homepage: http://engstroy.spbstu.ru/

Research article

UDC 691-408.66

DOI: 10.34910/MCE.114.8

Influence of electromagnetic field on characteristics of crushed materials

***R.A. Ibragimov*[1] ✉ , *E.V. Korolev*[2]**

[1] *Kazan State University of Architecture and Engineering, Kazan, Russia*

[2] *Saint Petersburg State University of Architecture and Civil Engineering, Saint Petersburg, Russia*

✉ *rusmag007@yandex.ru*

Keywords: cements, energy efficiency, specific surface area, electromagnetic field

Abstract. This paper describes the findings of a study into the impact of the magnitude of induction and the frequency of rotation of an electromagnetic field on the properties of materials (Portland cement, gypsum plaster, limestone), which are treated in the vortex layer machines. The effects were assessed based on the following criteria: 1) the location of the maximum values of the specific surfaces in the factor space as determined by the Tovarov method based on the BET method and the temperature of the model powders following treatment in a vortex layer machine; 2) the symbasis of the change in the values of the specific surface as determined by the BET method and the temperature of the powders following activation. Theoretical and experimental studies have been used as a basis for putting forward the concept of treatment in vortex layer machines. The essence of the concept lies in boosting the defectiveness of particles (i.e. accumulation of defects) followed by defects emerging and particles dispersing. The maximum values of specific surfaces and of the temperature of powder upon activation can be obtained at an electromagnetic field rotation frequency of 66 Hz while the material being treated is mechanically activated at an electromagnetic field induction value of 0.21 T with Portland cement, 0.22 T with gypsum plaster and 0.23 T with limestone. A classification to define the susceptibility of the mineral component to treatment inside vortex layer machines has been proposed.

Citation: Ibragimov, R.A., Korolev, E.V. Influence of electromagnetic field on characteristics of crushed materials. Magazine of Civil Engineering. 2022. 114(6). Article No. 11408. DOI: 10.34910/MCE.114.8

1. Introduction

Materials science in the domain of construction states that a variety of mills, dispersants, disintegrators and other kinds of devices are employed to obtain mineral components of the needed dispersed composition or specific surface [1–3].

A material is destroyed under the action of various physical forces such as impact, abrasion or a combination of them. Grinding bodies are propelled by gravity, or by centrifugal forces [4, 5].

Grinding media move at different rates depending on the type of machine used. It is well-known that materials behave quite differently under quasi-static and dynamic loadings. When loaded at a high rate, a material is able to withstand a significantly higher load provided a corresponding static impact is applied [6–7].

Recently, electromagnetic disintegrating machines have found widespread use [8]; a vortex layer machine being one of them. The electromagnetic field generated by an electromagnetic disintegrating machine sets in motion ferromagnetic bodies inside the chamber in a chaotic order [9]. Determinations of the quantitative properties of disintegrating machines normally take into account the impact force, the time of grinding, and the energy intensity of the process while the effect which the electromagnetic field produces on the substance is absolutely ignored [10–12].

It was established that a weak magnetic field with B ≈ 1 T induction barely affects the structure and properties of non-magnetic solid bodies [13]. With that said, the magnetic field has been found to affect the mobility of dislocations in the absence of an external mechanical load at B < 1 Tl on NaCl single crystals [14]. While investigating the mobility of edge dislocations in NaCl and LiF crystals, the authors [15] witnessed a 4.5 – fold decrease in the dynamic inhibition coefficient of dislocations under the action of an electron beam (pulsed magnetic field). The effect of a magnetic field reduces micro-hardness in NaCl single crystals. However, this process is reversible with a relaxation time of up to 18 hours [16].

The paper [17] indicates that by varying the parameters of the electromagnetic field during a grinding process one can set not only the average size of the particles but also the degree of uniformity of the powder.

An equation has been proposed to outline the elastic precursor of an elastic-plastic wave which forms under pulsed action in the paper [18, 19]. The equation reads as follows:

$$\sigma_y = \sigma_* + \left(\rho c \nu_p - \sigma_*\right)\exp\left(-2A\mu_0 S\left(x/c\right)\right) \quad (1)$$

(here x is the coordinate; c is the longitudinal velocity of sound; σ_* is the dynamically equilibrium value of the Hugoniot elastic limit; $A = b^2 N_0 / B$; $S = 2\mu_0 / 3\rho c^2$; μ_0 is the initial modulus of elasticity; ρ is the density of matter; b is the Burgers vector; N_0 is the initial density of mobile dislocations; B is the retardation constant of dislocations an analysis of which shows that with all other things being equal the decay rate of the elastic precursor goes down as the B coefficient decreases:

$$\frac{d\sigma_y}{dB} = -\frac{2\sigma_* b^2 N_0 \mu_0 S\left(x/c\right)}{x^2 \exp\left(2A\mu_0 S\left(x/c\right)\right)}. \quad (2)$$

The analysis of research and development information shown here suggests that vortex layer machine treatments must demonstrate effects which reveal the contributions of the electromagnetic field to grinding of material along with resulting physical limitations which impair the efficiency of vortex layer machine treatments.

This paper aims to determine the effect which electromagnetic field properties produce on the degree of change in the specific surface of treated materials. This is achieved by mathematical planning of experiments.

2. Methods, materials and equipment used in this study

2.1. Materials and objects of research

The following materials have been selected as models:

1. Portland cement I 42.5 produced by the Novotroitsky cement plant. The product meets the requirements under Russian State Standard GOST 31108-2016. The Portland cement in question features the following mineralogical composition: C_3S – 64–65 %, C_2S – 11–13 %, C_3A – 5–6 %, C_4AF – 14–15 %;

2. Limestone from the Bondyuzhsky deposit (Mendeleevsk, Republic of Tatarstan);

3. Gypsum plaster (brand G-5 BII) (β-semihydrate) produced by ZAO "Samara Gypsum Plant". The product conforms to Russian State Standard GOST 125-2018.

The specific surface of the initial Portland cement was 375.5±16.75 m^2/kg (as per Tovarov) and 1015±20.3 m^2/kg (under the BET method) with an average particle size of 5.15±0.21 microns.

Limestone was ground with material with a fraction of 0.315–0.63 mm picked for the study. The specific surface of the fraction was 6.4±0.3 m^2/kg (as per Tovarov) and 21.4±1 m^2/kg (under the BET method) with an average particle size of 380±10 microns.

The specific surface of the gypsum plaster was 260±11.75 m^2/kg (as per Tovarov) and 754±15.1 m^2/kg (under the BET method) with an average particle size of 8.7±0.26 microns.

Portland cement, gypsum plaster and limestone underwent treatment in a vortex layer machine manufactured by OOO "Regionmettrans"; model 297. The paper [20, 21] presents a typical vortex layer machine design.

The specific surface was determined by relying on the air permeability method using a PSH-9 device and the BET method (Nova 1200e Quantachrome analyzer).

The magnetic field induction was determined by a magnetometer with a Hall sensor.

A TemPro 300 pyrometer was used to measure the temperature of materials treated in the vortex layer machine. The device operates in a measurement range of 32 to 350 °C and offers a measurement accuracy of ±1.5 °C.

The duration of treatment by the vortex layer machine was assumed to be the same and amounted to five minutes in the case of Portland cement and limestone and three minutes in the case of gypsum plaster.

The effects observed as the materials were being treated in the vortex layer machine were assessed based on two criteria:

- location of the maximum values $S_{ud,T}$, $S_{ud,BET}$ and $T_{\max}$ in the factor space which determines the intensity of vortex layer machine treatment ($S_{ud,T}$ is the specific surface determined under the Tovarov method; $S_{ud,BET}$ is the specific surface determined by the BET method; $T_{\max}$ is the maximum heating temperature of material powder after having been treated in a vortex layer machine). The magnetic field induction $\left(X_1\right)$ and the electromagnetic field rotation frequency $\left(X_2\right)$ were the factors which determined the material treatment mode in the vortex layer machine;
- symbasis of the change $S_{ud,BET}\left(X_1, X_2\right)$ and $T_{\max}\left(X_1, X_2\right)$.

3. Results and Discussion

The criteria have been selected based on the following scientific hypothesis. In the process of electromagnetic mechanical activation, the treated substance is affected by both the mechanical shock effects of ferromagnetic particles and electromagnetic forces (the Lorentz force and the effect of electromagnetic field strength). However, a certain intensity may make the mechanical action of ferromagnetic bodies cause various defects which naturally results in the area of the phase interface growing. Given the specificity of the resulting defects, a change like this in the phase interface can be recorded through the specific surface area based on the BET method. The mechanical action which comes next causes defects, cracks and the destruction of particles in the material being treated. This naturally leads to increasing dispersion which can be recorded through the specific surface area based on the Tovarov method.

A material being treated in a vortex layer machine sees an increase in temperature. This impacts the effects which occur when an electromagnetic field is being applied to the substance of a material. In the case of dielectrics, an increase in temperature leads to a disruption in the orientation of the dipoles [22, 23], while crystals are exposed to a Peierls-Nabarro effect which consists in inhibited movement of dislocations [24–26]. Still, the contribution of the aforementioned effect is significant at low temperatures only. It is clear that the impact of temperature will be of extreme nature. A point of extremum reached should be followed a decrease in the level of defectiveness of the material being treated characterized by $S_{ud,BET}$. A change in the treatment mode (factors X_1 and X_2) should naturally lead to a virtually linear increase in the temperature of the material. It appears from the foregoing that certain values of the factors $X_{1,S}$ and $X_{2,S}$ cause a disruption in the symbasis of the way in which $S_{ud,BET}\left(X_1, X_2\right)$ and $T_{max}\left(X_1, X_2\right)$ divert from the variable factors. This point of the factor space once achieved means that the competing processes of the effects of the electromagnetic field and of the temperature on the defectiveness of the material have reached the same intensity.

The increasing effects of competing processes caused by temperature as a material is being treated in the vortex layer machine will indicate that the following condition has been fulfilled:

$$\frac{dS_{ud,BET}\left(X_1,X_2\right)}{dX_i}<\frac{dT_{\max}\left(X_1,X_2\right)}{dX_i} \quad (3)$$

The concept of vortex layer machine material treatment – an increase of particle defectiveness (up to $S_{ud,BET}\left(X_1,X_2\right)=\max$) → development of defects and dispersion of particles of the material being treated (up to $S_{ud,T}\left(X_1,X_2\right)=\max$) – indicates that an optimal mode of vortex layer machine material treatment ensuring its mechanical activation should be in the interval between the specified points of the factor space.

A two-factor composite (rotatable) plan is has been designed to test the concept with a quadratic model used:

$$Y\left(X_1,X_2\right)=b_0+b_1X_1+b_2X_2+b_{12}X_1X_2+b_{11}X_1^2+b_{22}X_2^2, \quad (4)$$

where b_i are the parameters of the experimental-statistical model.

The variable parameters included the magnetic field induction in the working chamber of the vortex layer machine $\left(X_1\right)$ with a parameter boundary of 0.06 T to 0.24 T, a variation interval of 0.09 T. The frequency of rotation of the electromagnetic field $\left(X_2\right)$ had a parameter boundary of 30 to 110 Hz and a variation interval of 40 Hz.

Under this concept the responses turned out to be $S_{ud,T}$, $S_{ud,BET}$ and $T_{\max}$.

An experiment planning matrix which shows the desired responses for model materials under examination is given in Table 1.

Table 1. Planning matrix and experiment results.

Plan point	Factor		Specific surface, m^2/kg (under the Tovarov method)	Specific surface area, m^2/kg (BET)	Average particle size, microns	Powder temperature after treatment, ºC
	X_1	X_2				
Portland cement						
1	0.06	30	460±22.0	1255±21.0	4.22±0.17	85
2	0.24	30	505±24.0	1405±24.0	3.90±0.17	90
3	0.06	110	385±18.0	1055±18.0	5.11±0.20	80
4	0.24	110	415±20.0	1160±19.5	4.69±0.18	82
5	0.02	70	550.0±26.0	1780±28.5	3.43±0.16	110
6	0.28	70	610.0±29.0	2075±37.2	3.09±0.12	120
7	0.15	13.43	410±20.0	1125±19.0	4.73±0.18	55
8	0.15	126.57	395±19.0	1095±18.5	5.28±0.21	45
9	0.15	70	580.0±28.0	1930±32.6	3.17±0.14	115
Gypsum plaster						
1	0.06	30	326±13.0	984±19.0	6.81±0.2	73
2	0.24	30	387±15.3	1124±22.5	5.85±0.17	79
3	0.06	110	265±10.6	792±15.8	8.55±0.25	67
4	0.24	110	295±11.8	904±18.1	7.67±0.23	72
5	0.02	70	439±17.6	1599±31.9	5.16±0.15	101
6	0.28	70	571±22.8	2132±42.6	3.96±0.12	111
7	0.15	13.43	286±11.4	859±17.2	7.92±0.23	49
8	0.15	126.57	275±11.0	832±16.6	8.23±0.25	41
9	0.15	70	505±20.2	1851±37.1	4.48±0.13	106
Limestone						
1	0.06	30	160±6.5	545±11.0	14.1±0.56	76
2	0.24	30	190±7.5	660±13.0	11.9±0.47	82
3	0.06	110	130±5.0	435±8.5	17.5±0.7	71
4	0.24	110	145±6.0	500±10.0	15.9±0.64	74

Plan point	Factor		Specific surface, m²/kg (under the Tovarov method)	Specific surface area, m²/kg (BET)	Average particle size, microns	Powder temperature after treatment, °C
	X_1	X_2				
5	0.02	70	215±8.5	885±17.5	10.8±0.43	103
6	0.28	70	280±11.0	1180±23.5	8.2±0.33	109
7	0.15	13.43	140±5.5	475±9.5	16.3±0.65	47
8	0.15	126.57	135±5.5	460±9.0	17.1±0.68	40
9	0.15	70	245±10.0	1025±20.5	9.3±0.37	107

Values of the parameters of the experimental and statistical models (4) are given in Table 2.

Table 2. Coefficients of the parameters of the obtained experimental and statistical models.

Property	Model parameter					
	b_0	b_1	b_2	b_{12}	b_{11}	b_{22}
Portland cement						
Specific surface area under the Tovarov method, m²/kg	580	20	–23.3	–3.8	–12.5	–101.3
Specific surface under the BET method, m²/kg	1935	85.1	–60.3	–11.3	–74.2	–487.3
Average particle diameter, microns	3.2	–0.1	0.3	-0.03	0.1	1
Powder temperature after treatment, °C	115	2.6	–3.4	–0.8	0.4	–32
Gypsum plaster						
Specific surface area under the Tovarov method, m²/kg	505	34.7	–21.1	–7.8	–18.6	–130.9
Specific surface under the BET method, m²/kg	1851	132.2	–56	–6.5	–92.1	–602.1
Average particle diameter, microns	4.5	–0.4	0.5	0.02	0.2	2
Powder temperature after treatment, °C	106	3.1	–3	–0.3	–0.7	–31.2
Limestone						
Specific surface area under the Tovarov method, m²/kg	245	17.1	–10.3	-3.8	–7.8	–62.8
Specific surface under the BET method, m²/kg	1025	74.7	-36.4	–12.5	–50	–332.5
Average particle diameter, microns	9.3	–0.9	1	0.1	0.5	4.1
Powder temperature after treatment, °C	107	2.2	–2.9	–0.8	–0.3	–31.5

The analysis given in Table 2 shows that in the case of all of the materials under examination, the maximum values $S_{ud,T}$, $S_{ud,BET}$ and $T_{\max}$ are in the factor space on the same line at X_2 = 66 Hz.

Typical graphs $S_{ud,BET} = f(X_1)$, $S_{ud,T} = f(X_1)$ and $T_{max} = f(X_1)$ are shown in Fig. 1 (at X_2 = 66 Hz) which also shows the location of the maximum values of these dependencies with their actual values presented in Table 3. The coordinate $X_{1,S}$ is the boundary X_1 which when surpassed leads to a disruption in the symbasis of the change of $S_{ud,BET} = f(X_1)$ and $T_{\max} = f(X_1)$ has been determined based on the following formula:

$$X_{1,s} = \frac{2b_{11}}{b_1 + b_{12}X_2} \tag{5}$$

and the condition (3) can be converted to appear as follows:

$$\frac{k_s X_1 + 1}{k_T X_1 + 1} \le 1, \tag{6}$$

where $k_i = 2b_{11,i} / \left(b_{1,i} + b_{12,i} X_2\right)$; indexes "$s$" and "$T$", respectively, for $S_{ud,BET} = f\left(X_1\right)$ and $T_{max} = f\left(X_1\right)$; $X_2 = \text{const.}$

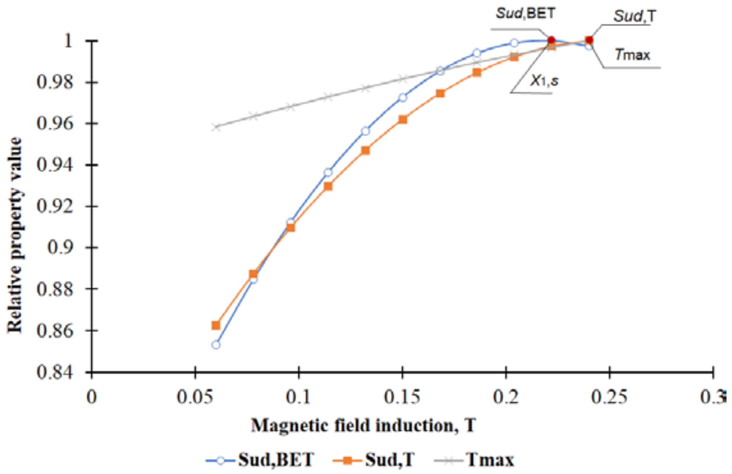

Figure 1. A typical graph of dependencies of $S_{ud,BET} = f\left(X_1\right)$, $S_{ud,T} = f\left(X_1\right)$ and $T_{max} = f\left(X_1\right)$.

The data shown in Fig. 1 and Table 3 support the validity of the concept of vortex layer machine material treatment: the temperature of the material powder goes up in the process of treatment; the dependency $T_{\max} = f\left(X_1\right)$ is rectilinear; accumulation of defects is of extreme nature caused by development of defects resulting in an increase in the dispersion of the powder of the material being treated. This is also evidenced by the location of the maximum values $S_{ud,BET}$ and $S_{ud,T}$:

$$\left|X_1\right|_{S_{ud,T}} > \left|X_1\right|_{S_{ud,BET}}. \tag{7}$$

Table 3. Coordinates of points in the factor space.

Material	Coordinates of points in the factor space								
	Properties								
	$S_{ud,BET}$		$S_{ud,T}$		$T_{\max}$		$X_{1,S}$, T	$X_{2,S}$, Hz	Condition (3)
	X_1, T	X_2, Hz	X_1, T	X_2, Hz	X_1, T	X_2, Hz			
Portland cement	0.204	66	0.222	66	0.24	66	0.230		+
Gypsum plaster	0.213	66	0.24	66	0.24	66	0.231	66	+
Limestone	0.222	66	0.24	66	0.24	66	0.233		+

The analysis of experimental and statistical models demonstrates that the condition (3) is fulfilled. The mechanically activated mineral component requires that two conditions be fulfilled: an increase in the dispersion (1) and the defectiveness (2) of the particles of the powder being treated. Under the concept, these conditions correspond to the equality:

$$S_{ud,BET}\left(X_1\right) = S_{ud,T}\left(X_1\right). \tag{8}$$

The equality (8) for Portland cement is met at $X_{1,opt}$ = 0.21 T, for gypsum plaster – at $X_{1,opt}$ = 0.22 T, and for limestone at $X_{1,opt}$ = 0.23 T.

An analysis of the effect of the mode selected on accumulation of defects $S_{ud,BET} = f\left(X_1\right)$ allows the susceptibility parameter which is calculated by the formula:

$$K_{ac} = \frac{S_{ud,BET}\left(X_{1,\min}\right)}{S_{ud,BET,\max}}, \quad (9)$$

($S_{ud,BET,\max}$ is the maximum value of the specific surface area as determined by the BET method) to arrange the mineral components in question in the following order:

Limestone > gypsum plaster > Portland cement.

This classification differs from the other classifications which are based on:

– the criteria of iron ion content and/or magnetic susceptibility;
– the criterion of grind ability.

Under the first classification the materials in question can be arranged in the following order based on their properties (Table 4):

Portland cement > Gypsum plaster > Limestone,

under the second classification:

Gypsum plaster > Limestone > Portland cement.

Table 4. Some properties of the materials under examination

Material name	Type of substance	The content of iron ions in fixed form	Magnetic susceptibility, χ
Portland cement	Paramagnetic	+	$45 \cdot 10^{-5}$
Gypsum plaster	Paramagnetic	–	$12 \cdot 10^{-5}$
Limestone	Diamagnetic	–	$-300 \cdot 10^{-5}$

Note. The "+" symbol indicates presence, the "-" symbol indicates absence or the need for further research.

The classification difference shown here serves to confirm once again that the electromagnetic field and the temperature produce a mutual effect when materials are being treated in a vortex layer machine.

4. Conclusion

1. The paper proposes and justifies a concept of material treatment by vortex layer machines which consists in a consistent increase in the defectiveness of particles (up to $S_{ud,BET}\left(X_1, X_2\right) = \max$) with subsequent development of defects and dispersion of particles in the material being treated (up to $S_{ud,T}\left(X_1, X_2\right) = \max$). However, the temperature of material powder when it is being treated rises almost linearly accompanied by extreme kinetics of defect accumulation resultant from development of defects which gives rise to an increase in the dispersion of the powder of the material being treated. The electromagnetic field and temperature have been confirmed to have competing effects in the range of vortex machine treatment parameters under examination.

2. The effects of the magnitude of the induction value and the frequency of rotation of the electromagnetic field on the specific surface and the temperature of the powders of Portland cement, gypsum plaster and limestone after being treated in a vortex layer machine have been determined. It has established that the highest values of the specific surface are achieved at a frequency of rotation of electromagnetic field of 66 Hz while the conditions to increase the dispersion and defectiveness of the particles of the powder being treated are fulfilled at a value of electromagnetic field induction of 0.21 T with Portland cement; 0.22 T – with gypsum plaster and 0.23 T with limestone.

3. The paper proposes a classification of the susceptibility of mineral components to treatment in vortex layer machines (per criterion $S_{ud,BET}$ in decreasing order): Limestone > gypsum plaster > Portland cement.

References

1. Mucsi, G. A review on mechanical activation and mechanical alloying in stirred media mill. 148. Institution of Chemical Engineers, 01-08-2019.
2. Acar, I., Acisli, O. Mechano-chemical surface modification of calcite by wet-stirred ball milling. Applied Surface Science. 2018. 457. Pp. 208–213. DOI: 10.1016/j.apsusc.2018.06.247

3. Boldyreva, E. Mechanochemistry of inorganic and organic systems: What is similar, what is different? Chemical Society Reviews. 2013. 42 (18). Pp. 7719–7738. DOI: 10.1039/c3cs60052a. URL: https://pubmed.ncbi.nlm.nih.gov/23864028/ (date of application: 20.03.2021).
4. Trejbal, J. Mechanical properties of lime-based mortars reinforced with plasma treated glass fibers. Construction and Building Materials. 2018. 190. Pp. 929–938. DOI: 10.1016/j.conbuildmat.2018.09.175
5. Arizzi, A., Cultrone, G. Comparing the pozzolanic activity of aerial lime mortars made with metakaolin and fluid catalytic cracking catalyst residue: A petrographic and physical-mechanical study. Construction and Building Materials. 2018. 184. Pp. 382–390. DOI: 10.1016/j.conbuildmat.2018.07.002
6. Morozov, V.A., Petrov, Y.V., Sukhov, V.D. Experimental Evaluation of Structural and Temporal Characteristics of Material Fracture Based on Magnetic Pulse Loading of Ring Samples. Technical Physics. 2019. 64 (5). Pp. 642–646. DOI: 10.1134/S1063784219050165
7. Atroshenko, S.A., Morozov, V.A., Kats, V.M., Gribanov, D.A., Petrov, Y. V. Rupture of copper rings by a magnetic-pulse method over a wide range of loading times. Procedia Structural Integrity. 2018. 13. Pp. 1373–1377. DOI: 10.1016/j.prostr.2018.12.287
8. Khaydarov, B., Suvorov, D., Pazniak, A., Kolesnikov, E., Gorchakov, V., Mamulat, S., Kuznetsov, D. Efficient method of producing clinker-free binding materials using electromagnetic vortex milling. Materials Letters. 2018. 226. Pp. 13–18. DOI: 10.1016/j.matlet.2018.05.016
9. Ibragimov, R.A., Korolev, E.V., Deberdeev, T.R., Leksin, V.V. Efficient complex activation of Portland cement through processing it in the vortex layer machine. Structural Concrete. 2019. 20 (2). Pp. 851–859. DOI: 10.1002/suco.201800008
10. Ibragimov, R.A., Korolev, E.V., Kayumov, R.A., Deberdeev, T.R., Leksin, V.V., Sprince, A. Efficiency of activation of mineral binders in vortex-layer devices. Magazine of Civil Engineering. 2018. 82 (6). Pp. 191–198. DOI: 10.18720/MCE.82.17
11. Całus, D., Makarchuk, O. Analysis of interaction of forces of working elements in electromagnetic mill. Przeglad Elektrotechniczny. 2019. 95 (12). Pp. 64–69. DOI: 10.15199/48.2019.12.12
12. Ogonowski, S., Ogonowski, Z., Pawełczyk, M. Multi-objective and multi-rate control of the grinding and classification circuit with electromagnetic mill. Applied Sciences (Switzerland). 2018. 8 (4). DOI: 10.3390/app8040506
13. Davydov, V.N., Karankevich, O.A. Application of the Onsager Principle to the Polar-axial Phenomena in Crystal Physics. Russian Physics Journal. 2019. 61 (10). Pp. 1922–1932. DOI: 10.1007/s11182-019-01619-w
14. Zhigachev, A.O., Rodaev, V.V., Umrikhin, A.V., Golovin, Y.I. The effect of silica content on microstructure and mechanical properties of calcia-stabilized tetragonal zirconia polycrystalline ceramic. Ceramics International. 2019. 45 (1). Pp. 627–633. DOI: 10.1016/j.ceramint.2018.09.220
15. Darinskaya, E.V., Koldaeva, M.V., Alshits, V.I., Voloshin, A.E., Pritula, I.M. Threshold Effects of the Magnetic Influence on the Microhardness of KDP Crystals. JETP Letters. 2019. 110 (4). Pp. 279–283. DOI: 10.1134/S0021364019160045
16. Alshits, V.I., Darinskaya, E.V., Koldaeva, M.V., Petrzhik, E.A. Paradoxes of the influence of small Ni impurity additions in a NaCl crystal on the kinetics of its magnetoplasticity. Journal of Experimental and Theoretical Physics. 2016. 122 (1). Pp. 118–130. DOI: 10.1134/S1063776115130014
17. Egorov, I.N., Egorova, S.I., Kryzhanovsky, V.P. Particle size distribution and structural state analysis of mechanically milled strontium hexaferrite. Materials Science Forum. 2019. 946 MSF. Pp. 293–297. DOI: 10.4028/www.scientific.net/MSF.946.293
18. Morozov, V., Kats, V., Savenkov, G., Lukin, A. Mechanisms of fracture of ring samples made of FCC metals on loading with magnetic-pulse method. AIP Conference Proceedings. 2018. 1959. DOI: 10.1063/1.5034753
19. Zaychenko, O.K., Morozov, V.A. Building a stress calculation model for dynamic deformation of metal rings under magnetic loads. Journal of Physics: Conference Series. 2019. 1203 (1). DOI: 10.1088/1742-6596/1203/1/012018
20. Wołosiewicz-Głąb, M., Foszcz, D., Ogonowski, S. Design of the electromagnetic mill and the air stream ratio model. IFAC-PapersOnLine. 2017. 50 (1). Pp. 14964–14969. DOI: 10.1016/j.ifacol.2017.08.2554. URL: www.sciencedirect.com (date of application: 20.03.2021).
21. Ogonowski, S., Wołosiewicz-Gł, M., Ab, Ogonowski, Z., Foszcz, D., Pawełczyk, M. minerals Comparison of Wet and Dry Grinding in Electromagnetic Mill. 2018. DOI: 10.3390/min8040138. URL: www.mdpi.com/journal/minerals (date of application: 20.03.2021).
22. Poplavko, Y.M. Dielectrics. Electronic Materials. Elsevier, 2019. Pp. 287–408.
23. Poplavko, Y., Yakymenko, Y. Physical nature of crystal internal polarity. Functional Dielectrics for Electronics. Elsevier, 2020. Pp. 1–49.
24. Edagawa, K., Kamimura, Y., Iskandarov, A.M., Umeno, Y., Takeuchi, S. Peierls stresses estimated by a discretized Peierls–Nabarro model for a variety of crystals. Materialia. 2019. 5. Pp. 100218. DOI: 10.1016/j.mtla.2019.100218
25. Boldyrev, V.V. Mechanochemical processes with the reaction-induced mechanical activation. Chemo-mechanochemical effect. 67 (6). Springer, 01-06-2018.
26. Stroganov, V., Sagadeev, E., Ibragimov, R., Potapova, L. Mechanical activation effect on the biostability of modified cement compositions. Construction and Building Materials. 2020. 246. Pp. 118506. DOI: 10.1016/j.conbuildmat.2020.118506

Information about authors:

Ruslan Ibragimov,
PhD in Technical Science
ORCID: https://orcid.org/0000-0001-8879-1190
E-mail: rusmag007@yandex.ru

Evgeny Korolev,
Doctor in Technical Science
ORCID: https://orcid.org/0000-0003-0815-4621
E-mail: korolev@nocnt.ru

Received 31.03.2021. Approved after reviewing 23.11.2021. Accepted 26.11.2021.